Reinforcement of Soy Polyol-Based Rigid Polyurethane Foams by Cellulose Microfibers and Nanoclays

Min Zhu, Sanchita Bandyopadhyay-Ghosh, Mustafa Khazabi, Hui Cai, Carlos Correa,* Mohini Sain

Centre for Biocomposites and Biomaterials Processing, University of Toronto, Toronto, Ontario, Canada M5S 3B3

Received 6 July 2010; accepted 21 August 2011
DOI 10.1002/app.35511
Published online 6 December 2011 in Wiley Online Library (wileyonlinelibrary.com).

ABSTRACT: Water-blown rigid polyurethane foams from soy-based polyol were prepared and their structure–property correlations investigated. Cellulose microfibers and nanoclays were added to the formulations to investigate their effect on morphology, mechanical, and thermal properties of polyurethane foams. Physical properties of foams, including density and compressive strength, were determined. The cellular morphologies of foams were analyzed by SEM and X-ray micro-CT and revealed that incorporation of microfibers and nanoclays into foam altered the cellular structure of the foams. Average cell size decreased, cell size distribution narrowed and number fractions of small cells increased with the incorporation of microfibers and nanoclays into the foam, thereby altering the foam mechanical properties. The morphology and properties of nanoclay reinforced polyurethane foams were also found to be dependent on the functional groups of the organic modifiers. Results showed that the compressive strengths of rigid foams were increased by addition of cellulose microfibers or nanoclays into the foams. Thermogravimetric analysis (TGA) was used to characterize the thermal decomposition properties of the foams. The thermal decomposition behavior of all soy-based polyurethane foams was a three-step process and while the addition of cellulose microfibers delayed the onset of degradation, incorporation of nanoclays seemed to have no significant influence on the thermal degradation properties of the foams as compared to the foams without reinforcements. © 2011 Wiley Periodicals, Inc. J Appl Polym Sci 124: 4702–4710, 2012

Key words: renewable resources; nanocomposites; polyurethanes; structure–property relations

INTRODUCTION

Polyurethane (PU) foams, which are used extensively in many industries, from construction to automobiles, insulation to furniture, account for the largest market among polymeric foams in the world.[1] Derivatives from petroleum are the major raw materials for the polyurethane foams. PU foams are prepared by reacting polyol with an isocyanate, in which the reacting mixture is foamed using one or more blowing agents and surfactants. Efforts to use alternative resources to replace finite petroleum for making polyurethane foams have been accelerated in recent years. Vegetable oil-based polymers are gaining popularity due to some attractive properties related to the specific structure of oils, as well as concerns about environment and sustainability.[2] Because of being more environment-friendly and renewable, polyols derived from vegetable oils have a great potential to replace the petroleum resource. Vegetable oils have unsaturations in their chemical structures and can be converted to polyols, a precursor for polyurethane foam through the introduction of hydroxyl functional groups into these sites of unsaturation.[2] Thus far, vegetable oil-derived polyols have been used to replace or partially replace petroleum polyols to synthesize rigid and flexible polyurethane foams. Vegetable oils, including soybean oil, canola oil, palm oil, and rape seed oil were converted to polyol and further to produce polyurethane foams.[3–9] Soybean oil is the most attractive raw material in North America since it combines stability and low price with a relatively high degree of unsaturation. Cellular morphology and mechanical properties of the PU foams are affected significantly by the foam fabrication method and polyol hydroxyl number. PU foams may have open or closed cells. Dimensional stability of cured foams is governed by the fraction of open cells. In rigid polyurethane foams used for thermal insulation, a large fraction of the cells (>95%) should be closed to ensure that the low thermal conductivity blowing agent remains entrapped within the foam.[4]

With increasing interest and broad range of applications, enhancement of mechanical properties of PU

Correspondence to: S. Bandyopadhyay-Ghosh (sanchita.bandyopadhyayghosh@utoronto.ca).
*On Leave from University Sao Francisco, Brazil

foams is of important consideration as they often suffer from poor mechanical properties. Incorporation of lignocellulosic materials in polyurethane foam could provide a powerful approach for the enhancement of its mechanical properties and the introduction of biodegradability to the foam products. There have been some reports of using lignocellulosic materials (molasses, wood fiber etc.) with petroleum based polyol for making PU in the form of sheet, foam and composites.[10–12] In this respect it would be interesting to study the reinforcing potential and morphology control of cellulose microfibers in soy polyol derived rigid polyurethane foam.

Nowadays, nanocomposites made from PU foams are also attracting great interest because they offer a great potential to exhibit superior properties when compared to pure polymers and conventional filled composites. The main advantages are high modulus and strength, increased thermal stability and flame retardancy.[13–15] Plate-like layered silicate clays such as montmorillonite (MMT) are commonly used as reinforcements or fillers. These layered silicate clays are a type of 2 : 1 layered smectite clay mineral with a sheet-like structure. The gaps between layers are called the interlayer or gallery. Isomorphous substitution between galleries results in negative charges on the clay surfaces that are neutralized by exchangeable cations such as Na^+, K^+, or Ca^{2+} ions inside the galleries.[16–20] Previous work has also shown that nanoclays in PU foams may act as foam openers.[4]

Although, there have been previous researches concerning various PU foam/nanoclay systems, to the best of our knowledge, there are no reports regarding the effect of cellulose microfiber and layered nanoclays on structure-property relationships of soy foam. In this study, water-blown rigid PU foams from soy-based polyol were prepared and the effect of the addition of cellulose microfibers and nanoclays on the foam morphologies and properties was investigated. The objective of this research is to improve foam properties by incorporating cellulose microfibers and nanoclays reinforcements.

MATERIALS AND METHODS

Materials

Soy-polyol R3-170 used in this study was supplied by Urethane Soy System Company (Volga, SD) with a hydroxyl number of 170. Isocyanate PAPI-27 was obtained from Dow Chemical (Midland, MI). Surfactant (Dabco® DC 5357) and catalysts (Dabco® T 12) and (Dabco® 33 LV) were obtained from Air Products and Chemicals (Allentown, PA). Distilled water was used as the blowing agent. Cellulose microfibers were obtained by refining a commercial pulp in a mechanical wood refiner Thomas-willey Laboratory Mill (Philadelphia, PA) and passing through 40 mesh sieve. Commercial nanoclays Cloisite Na^+, 93A and 30B were obtained from Southern Clay Products. Cloisite Na^+ is a natural montmorillonite (d spacing = 11.7 Å), modified with a methyl, dehydrogenated tallow quaternary ammonium salt (d spacing = 23.6 Å), while Cloisite 30B is a natural montmorillonite modified with a methyl, tallow, bis-2-hydroxyethyl, quaternary ammonium salt (d spacing = 18.5 Å).

TABLE I
Formulation for Water-Blown Rigid Soy-Based Polyurethane Foam

Component	Parts by weight (php)
Soy based polyol (hydroxyl number 170)	100
Water	2
Surfactant (Dabco® DC 5357)	1
Catalyst-I (Dabco® T 12)	0.4
Catalyst-II (Dabco® 33 LV)	0.4
Refined microfibre	0; 0.5; 1; 2
nano-particles	0; 2
PAPI-27 Index[a]	120

[a] The quantity of isocyanate was based on an isocyanate index, defined as the actual amount of isocyanate used over the theoretical amount of isocyanate required multiplied by 100.

Foam preparation

Table I shows the formulation for rigid soy polyurethane foams. The amount of each component was based on per hundred parts (php) by weight of total polyol. The amount of isocyanate was based on an index, defined as the actual amount of isocyanate used over the theoretical amount of isocyanate required according to the hydroxyl content of polyol and distilled water, multiplied by 100.

Microfibers and nanoclays were dried in an oven at 70°C for 24 h. The polyol and various amounts of different microfibers or nanoclays were weighed into a cup and mixed for 15 min under ambient conditions. Then other ingredients, except isocyanate, were added to the cup and mixed for 5 min. Then isocyanate was added and the mixing continued for additional 30 s. The mixtures were then quickly transferred to an open aluminum mold (18 cm × 8 cm × 8 cm). The foam was allowed to rise freely and cure for 2 h, after which the foam was removed from the mold. Further tests were done after the foam had aged at ambient conditions for 7 days.

Measurement of foam properties

Density of foam samples was measured according to ASTM D 1622-03. Compressive strength of foams was determined by Instron 3367 following ASTM D

1621-04a. Dimension of samples was 5 cm × 5 cm × 2.5 cm. The detailed procedures of measurement and calculation of foam parameters can be found in the aforementioned standards. Three samples per experiment per foam were tested and averages were reported.

Morphologies of soy based polyurethane foams

Scanning electron microscopy (SEM)

The rigid soy polyurethane foam samples were cut into rectangular slices (5 mm × 5 mm × 2 mm) in a direction parallel or perpendicular to the blowing direction. The top surface of each slice was sputter coated with gold. A Hitachi S-2500 scanning electron microscope (SEM, Tokyo, Japan) operated at 10-kV accelerating voltage was used to examine the surface of foams. At least five images were collected from each foam sample. The areas of cells were manually traced from the SEM micrographs using JMicroVision 1.2.7 software. Individual cell size (diameter) was then calculated by approximating the cells as circular shapes. Average cell diameter standard deviations were calculated from a survey of over 40 cells.

X-ray micro computed tomograph (Micro-CT) image analysis

The foam samples were examined using the high-resolution X-ray micro-CT system, SkyScan 1172 (SkyScan, Belgium). The X-ray source was an air-cooled, sealed microfocus X-ray tube with a focal spot size <8 μm. The X-ray tube was operated at 40 kV with no filter. The X-ray CCD (charge-coupled device) camera was based on a 2000 × 1048 12-bit cooled CCD sensor with fiber optic coupling to the X-ray scintillator. The system was controlled by a PC workstation running under Microsoft Windows XP Professional. Scanning of the specimens was done with 180-degree rotation around the vertical axis and a single rotation step of 0.4. After a half circle (180°) was completed, the entire set of radiographs was synthesized and reconstructed with the software NRecon. An automatic filter changer for beam-hardening compensation during reconstruction was used at a level of 35%. The reconstructed 2D images were saved as a stack of uncompressed 16-bit TIFF files. These TIFF files were then used to create a three-dimensional (3D) image of microstructure with the software Image-Pro Plus 6.1. The cell sizes were calculated with the same method described in the SEM micrographs.

Thermogravimetric analysis (TGA)

TGA analysis has been carried out using TA Instrument's TGA analyzer, model Q500, at a heating rate of 10°C min^{-1} in a nitrogen atmosphere.

RESULTS AND DISCUSSION

Morphologies of soy based polyurethane foams

Micrographs of soy polyurethane foams obtained from SEM as shown in Figures 1 and 2 were examined for morphological characterizations (at 100× magnifications). Most of the cells in all foams had closed cell structures. All foams exhibit polygon closed-cell structures with energetically stable pentagonal and hexagonal faces. The foam cells were in round shapes if observed in a direction perpendicular to the blowing direction of the foam. However, the cells of neat foam, foam with microfibers, Cloisite 93A and 30B were asymmetric when the foams were viewed in a direction parallel to the blowing direction. These foam cells were either in elliptical or energetically stable pentagonal and hexagonal shapes. Cells in foam with microfibers had the highest length/width ratio, while the cells of foam with Cloisite Na^+ had almost round shape when viewed in the direction parallel to the blowing direction. Figure 3 shows the cellular morphologies of neat foam, and foams reinforced with microfibers and Cloisite 93A obtained from X-ray micro CT.

The neat PU foam had fewer number of cells and larger cell sizes than reinforced PU foams. This can partly be due to the fact that both fiber and nanoclays can serve as nucleating agents for cell growth resulting into increased total numbers of nucleated cells and decreased cell sizes in the reinforced foams. Both X-ray micro-CT and SEM were used to calculate cell sizes. X-ray micro-CT images gave the similar results of the average cell size and distribution when compared to SEM micrographs. Figure 4 shows the images analyzed with X-ray micro-CT. Average cell diameter based on X-ray micro-CT images and standard deviations obtained are shown in Figure 5. The neat foam had the largest average cell size and broadest cell size distribution. With the incorporation of microfibers and nanoclays, foam average cell size decreased and cell size distribution narrowed. The foam with addition of Cloisite 93A had the smallest average cell size. The average cell size was 47% smaller than the neat foam and the cell size distribution was the narrowest. Figures 6 and 7 show the cell size distributions for of all foam samples. As shown in Figure 6, with incorporation of microfibers, the cell size distribution changed to a high percentage of small cells together with a low percentage of large cells. Among the nanoclay reinforcements, Cloisite 93A reinforced foam had the highest percentage of small cells together with the lowest percentage of large cells (Fig. 7). For example, of all the foam samples, only in Cloisite 93A, cell sizes less than 100 μm could be observed and the number of cells from 100 to

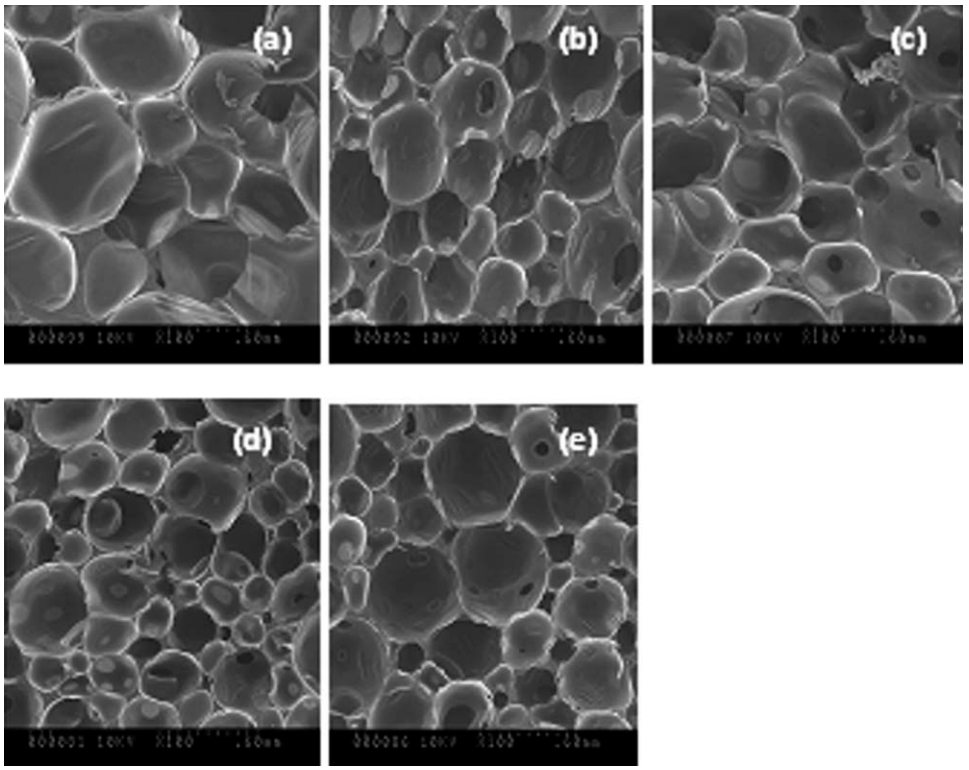

Figure 1 SEM micrographs when observed perpendicular to the blowing direction of foam (×100 magnifications): (a) neat foam; (b) foam with microfibers; (c) foam with Cloisite Na^+ (d) foam with Cloisite 93A; (e) foam with Cloisite 30B.

400 μm represents about 70% of the total cells. The number fraction of small cells (0–400 μm) among the nanoclay foams were found to vary in this order: Cloisite 93A > Cloisite 30B = Cloisite Na^+. This size distribution is connected with its physical properties and is discussed later.

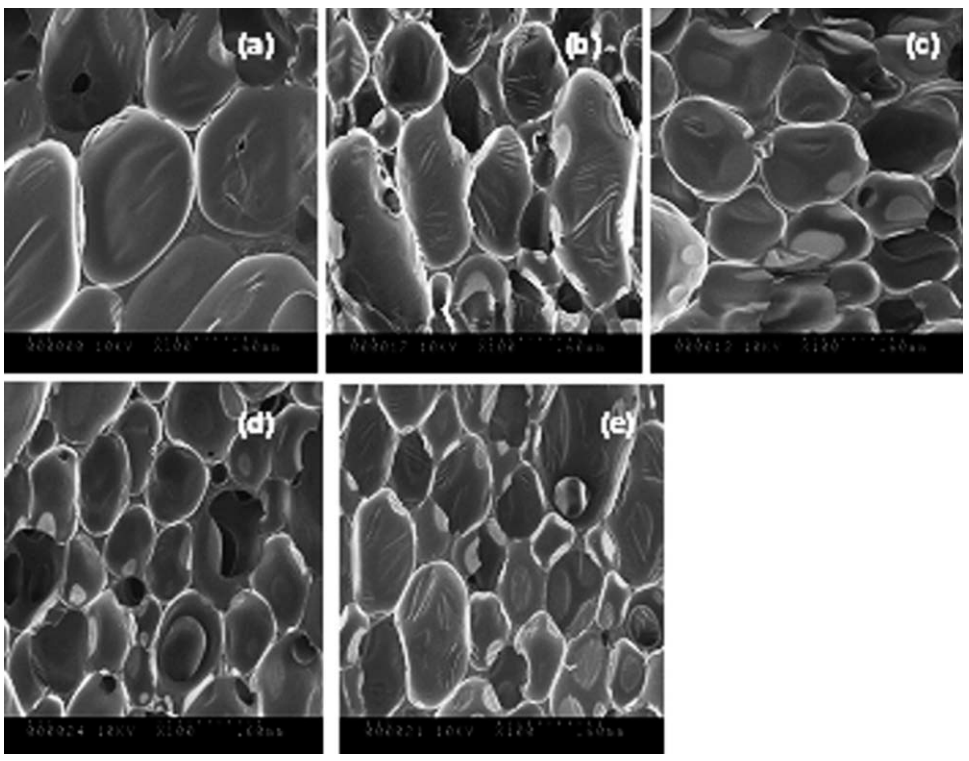

Figure 2 SEM micrographs when observed parallel to the blowing direction of foam: (a) neat foam; (b) foam with microfibers; (c) foam with cloisite Na+ (d) foam with Cloisite 93A; (e) foam with cloisite 30B.

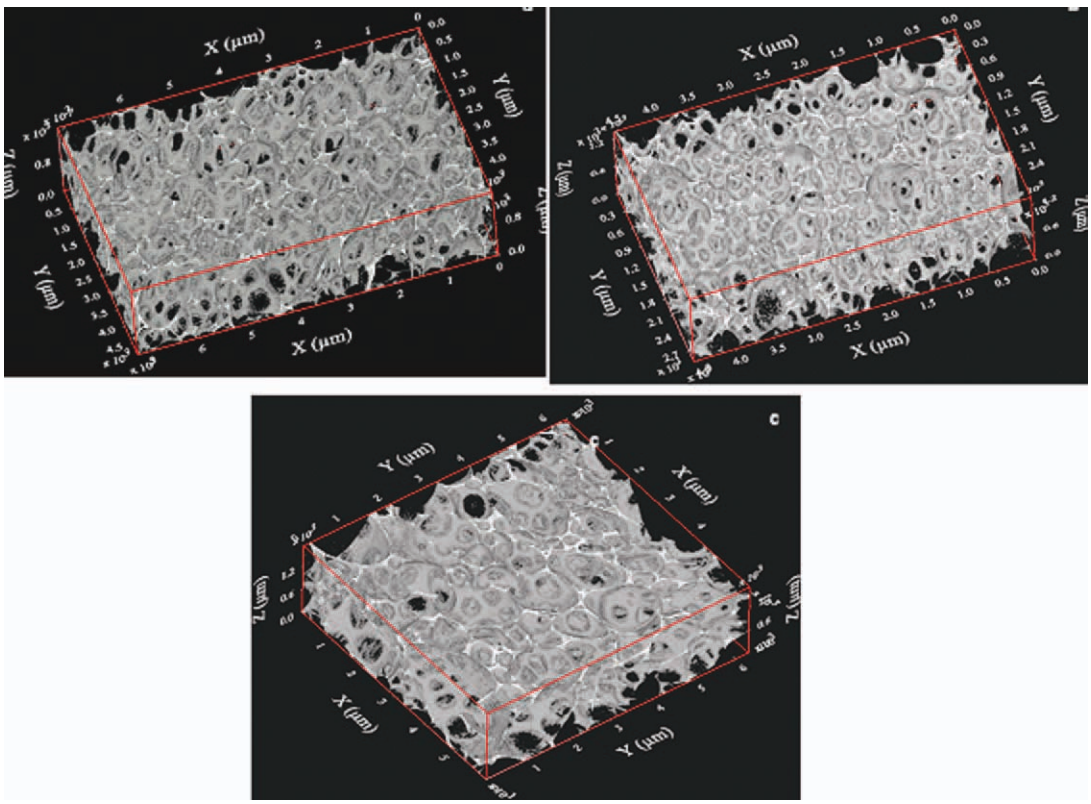

Figure 3 Three dimensional reconstruction of X-ray micro-CT images: (a) neat foam; (b) foam with microfibers; (c) foam with Cloisite 93A. [Color figure can be viewed in the online issue, which is available at wileyonlinelibrary.com.]

Structure–property correlations in reinforced rigid soy based polyurethane foams

Effects of the microfibers on density and compressive strength of rigid soy polyurethane foams are shown in Figure 8. Results show that incorporation of cellulose microfibers of 0.5, 1.0, and 2.0 php into foam had no significant influence on the density. This indicates that addition of microfibers at these levels did not change the behavior of foaming process. Compressive strengths increased significantly in the presence of microfibers of 1.0 and 2.0 php levels. Effects of nanoclays on density and compressive strength of rigid soy polyurethane foams are presented in Figure 9. Results show that densities of foams varied with different nanoclays. Adding cloisite NA^+ caused 58.9% increase in density, while addition of other nanoclays resulted in somewhat lesser changes in foam densities.

Owing to the fact that all nanoclay reinforced foams had different densities, to exclude the effect of density difference of the foam samples, the compressive strengths were normalized and specific strengths (compressive strength divided by the density) of the foam samples were used to compare the mechanical properties of the foams with different nanoclays. Figure 10 represents the specific compressive strengths of neat foam and nanoclay reinforced foam composites.

Normalized compressive strengths of foams reinforced with nanoclays increased compared to neat foam in all cases. The results indicate that Cloisite 93A imparted the highest improvement in the compressive strength, while Cloisite Na^+ and 30B had similar improvements compared to neat foam. The above results with nanoclays should be interpreted in terms of the difference in cell size distributions and chemical structures of the nanoclays as shown below.

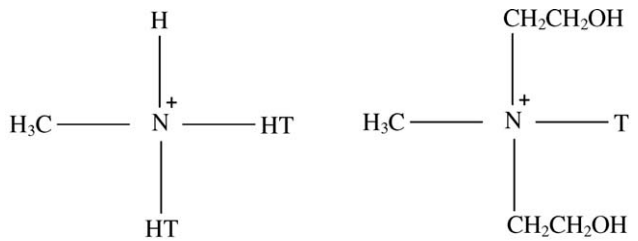

Cloisite 93A (HT is Hydrogenated Tallow)

Cloisite 30B (T is Tallow)

SEM and micro-CT studies and cell size analysis suggested that incorporation of microfibers and nanoclays into foam altered the cell size distribution of the foam. Consequently, the foam mechanical properties are likely to be affected by the change in cell sizes and by the distribution of small and large

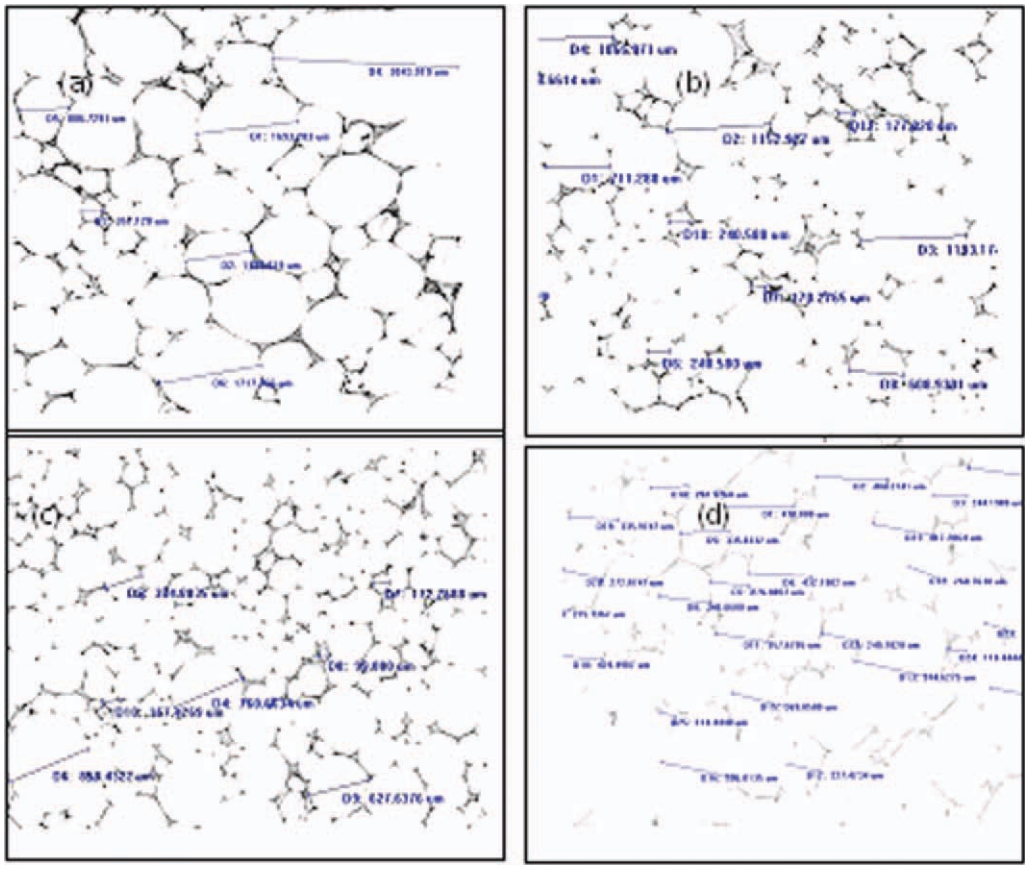

Figure 4 X-ray micro-CT images: (a) neat foam; (b) foam with microfibers; (c) foam with Cloisite 93A; (d) foam with Cloisite 30B. [Color figure can be viewed in the online issue, which is available at wileyonlinelibrary.com.]

cells. Comparing the results of compressive strengths and cell size distribution of the foams, there seems to be a correlation between them. Addition of microfiber or clays to the rigid foams decreased the cell sizes and number of large cells within the foam and increased the compressive strengths. Foam with Cloisite 93A had the smallest cell sizes and maximum number of small cells and provided the highest compressive strength. Similarly with other nanoclays, the compressive strength improvements followed the trend in accordance with cell sizes and their distributions.

The interfacial interactions among reinforcement materials and the polymer matrix is another crucial factor affecting the structure and properties of composites. The improvements in mechanical performance are mainly governed by the strength of reinforcement

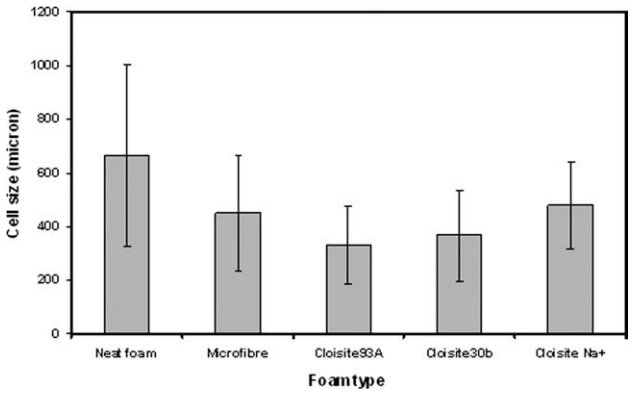

Figure 5 Average cell diameter of different type of soy based polyurethane foams and standard deviation based on X-ray micro-CT images when viewed perpendicular to blowing direction.

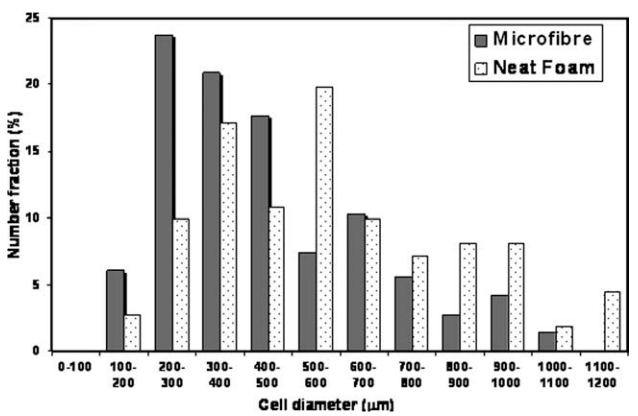

Figure 6 Number distribution of cell diameters of neat soy based polyurethane foams and microfiber reinforced soy-based foam.

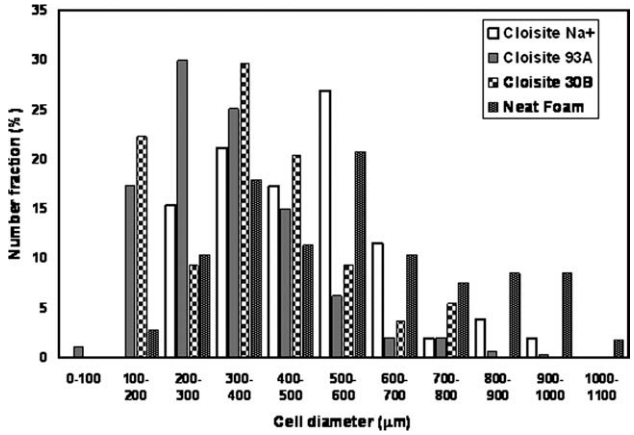

Figure 7 Number distribution of cell diameters of neat soy polyurethane foams and nanoclay reinforced soy foam.

fillers and strong interfacial interaction between the reinforcement surface and the matrix, as well as to the relatively uniform dispersion of the fillers. The performance improvement that were noticed both with cellulose microfibers or nanoclays showed a prominent reinforcing function that are in effect with also the results of uniform dispersion and strong interfacial interaction between the filler and semiinterpenetrating polyurethane matrix. Strong interfacial adhesion facilitates the transfer of stress. At the current loading levels of the microfibers it is evident that the microfibers did not show any strong tendency for self-aggregation which would result into a decrease in the effective active surface of the filler phase and weakened interfacial adhesion. The detailed analyses of interfacial effects are under investigation and will be reported in future publications. The improvements in mechanical performance with cellulose microfiber or nanoclays at the current loading levels can also mean no excess breakage of polyurethane network structure and absence of any microphase separation in the

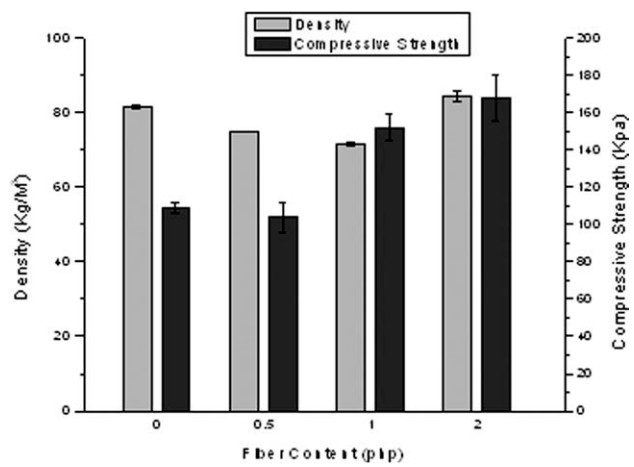

Figure 8 Effects of cellulose microfibers on density and compressive strength of soy polyurethane rigid foams.

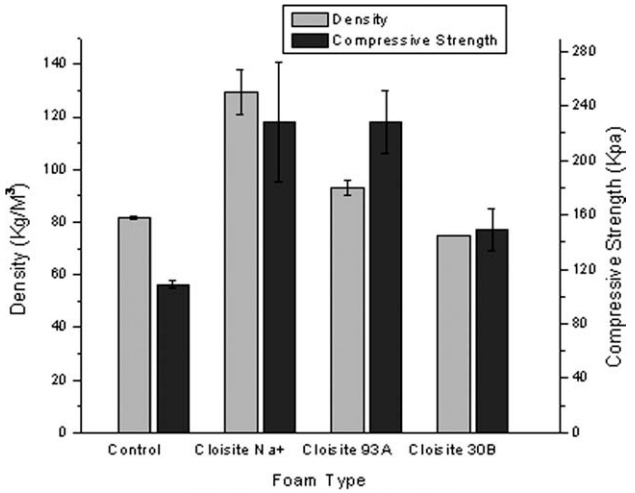

Figure 9 Effects of nano-clays on density and compressive strength of soy based polyurethane rigid foams.

composites, which would also inhibit enhancement of mechanical performance of the composites.[21]

In terms of chemical structure, Cloisite Na^+ being a natural montmorillonite with hydrated Na^+ in their galleries, is greatly hydrophilic and is incompatible with most nonpolar polymers. It can result in insufficient exfoliation and dispersion within the polymer. They can exist in clusters or aggregates of montmorillonite platelets and can act as stress concentrators. As a result, although, the foam compressive strengths were improved due to nanoscale reinforcement effect, the improvement was not significantly high with Cloisite Na^+.

However, with Cloisite 93A, the inorganic cations in the galleries are replaced with cationic surfactants with alkyl chains (methyl quaternary alkyl ammonium ions). This organophilic modification, replacing smaller cations with larger ones results in increasing interlayer distance and reduces the surface tension in the interlayer of clay, thereby increasing the ease of entry of the polyol. The methyl quaternary alkyl

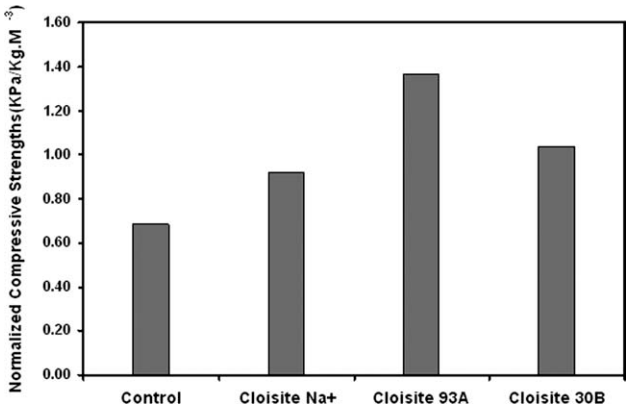

Figure 10 Specific compressive strengths of nanoclay reinforced rigid soy polyurethane foam.

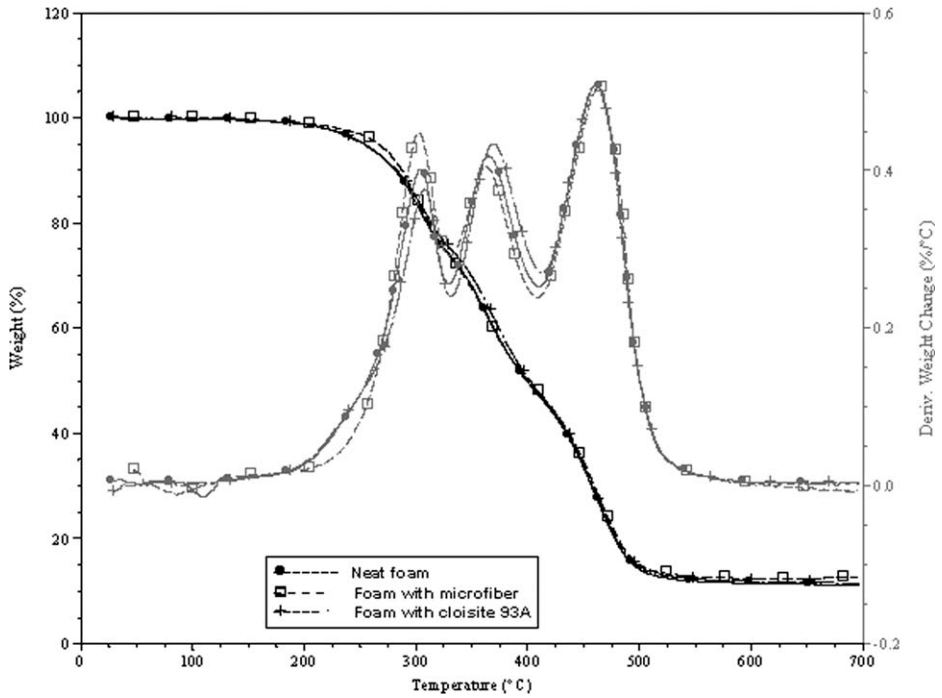

Figure 11 Thermograms of rigid soy-based polyurethane foams.

ammonium ions in Cloisite 93A therefore, play an important role as compatibilizer between hydrolphilic clays and hydrophobic polyol. Furthermore, the alkyl ammonium ions offer functional groups that can react with the polyol. Moreover, the functional groups supplied by ammonium ions can easily interact with the polyol matrix and enhance the strength of the interface between the clay and the polymer.[13,14] As a result a significant improvement in effective compressive strength was observed with incorporation of Cloisite 93A due to the synergistic effect of cell size distribution and chemical functionalities (Fig. 10).

Cloisite 30B on the other hand is modified with a hydroxyethyl quaternary ammonium salt. Because of the presence of hydroxyl (—OH) groups in Cloisite 30B (see structure above), upon exfoliation of the platelets, PU molecules can be grafted onto the clay surface through the reaction between the —NCO groups and the —OH groups on the Cloisite 30B. The tethered clay may interfere with the H-bond formation in PU causing a negative effect on the properties of PU nanocomposite foams, as it is well known that H-bond formation among urethane groups greatly contributes to the strength of PUs. Furthermore, the involvement of organoclays in the reaction could also affect the network structure formation of PU resulting into reduced cross-linking within the foam. The overall performance therefore depends on the competition between the positive effects of nanoclay on polymer reinforcement and foam morphology, and the negative effects on H-bond formation and network structure, a result that was reflected with compressive strength improvement of Cloisite 30B being slightly higher than Cloisite Na^+ but less compared to Cloisite 93A.

Thermogravimetric analysis of rigid soy based polyurethane foams

The thermograms presented in Figure 11 shows the thermal degradation behavior of rigid soy based polyurethane foams with or without microfibers or Cloisite 93A nanoclay in an atmosphere of nitrogen. There are three thermal transition peaks on derivative curve indicating that the thermal decomposition

TABLE II
Thermal Degradation Features of Soy-Based Polyurethane Rigid Foam Samples

	Degradation temperature (°C)					
Foam samples	T5	T50	First peak	Second peak	Third peak	Percentage of residue (%)
Neat foam	260 ± 8	402 ± 4	300 ± 4	357 ± 10	461 ± 1	13.0 ± 4.3
Foam with 2php fibre	270 ± 2	403 ± 3	303 ± 6	364 ± 4	462 ± 2	10.9 ± 1.4
Foam with 2php cloisite 93A	256 ± 3	400 ± 6	304 ± 6	367 ± 3	460 ± 1	11.4 ± 0.9

of the soy polyurethane foams is a three-step reaction. As shown in Table II, the first stage of weight loss was around 300°C, which seems to be caused by rupture of the urethane bonds.[3] Second stage of weight loss was at temperature about 360°C, and third stage of weight loss was at temperature around 460°C. Higher temperatures most likely represent the degradation of the polyol backbone. However, what caused the second and third stages of weight loss is still unclear. These thermograms are different from common thermal decomposition reaction of petroleum based polyurethane foams, which is a two-step reaction in nitrogen.[11] It was also observed that the 50 wt % decomposition temperatures of the foams (Table II) were not significantly affected by incorporation of microfibers or cloisite 93A. However, with addition of microfibers, the onset of thermal degradation (defined as the temperature when 5 wt % of the initial mass of the sample is lost) increased from 260°C in pure foam to 270°C in foam/microfiber composite. The observed thermal degradation behavior indicates that microfiber enhanced the onset temperature of degradation by acting as superior insulator and mass transport barrier to the volatile products generated during decomposition. However, no such improvement was observed with Cloisite 93A. This can be ascribed to the fact that the stacked layers in the nanocomposite could hold accumulated heat that could be used as a heat source to accelerate the decomposition process, in conjunction with the heat flow supplied by the outside heat source.[22] As a result, the improvement of thermal stability due to heat barrier effect was not realized when Cloisite 93A was used as reinforcement.

CONCLUSIONS

Soy polyol-based rigid polyurethane foams were prepared from natural oil feedstocks and the effect of cellulose microfiber and nanoclays on foam properties and morphologies were investigated. SEM and X-ray micro-CT observation of foams revealed modification in cellular structures owing to changes in kinetics of bubble nucleation and growth during the foaming process. Foam average cell size decreased, cell size distribution narrowed, and number fraction of small cells increased with the incorporation of microfibers and nanoclays into the foam. This along with the chemical interactions of nanoclays with urethane network structure significantly influenced the foam mechanical properties. The thermal decomposition of the soy polyurethane foams was a three-step reaction related to the decomposition of urethane bond and polyol backbone. Incorporation of microfibers into pristine foam delayed the onset degradation temperature from 260 to 270°C. However, with Cloisite 93A nanoclay, the overall thermal stability of the foams was not significantly affected. The results from this study therefore improved the overall understanding of the effect of microfiber and nanoclay reinforcement on soy based polyol rigid polyurethane foams and demonstrated that with suitable synthesis and dispersion techniques, the mechanical performances of soy polyurethane foam can be enhanced by modifying it with cellulose microfibers or nanoclays.

References

1. Ashida, K. Polyurethane and Related Foams: Chemistry and Technology; CRC Press: NY, 2006.
2. Petrovic, Z. S. Polym Rev 2008, 48, 109.
3. Guo, A.; Javni, I.; Petrovic, Z. J Appl Polym Sci 2000, 77, 467.
4. Harikrishnan, G.; Umasankar, P. T.; Khakhar, D. V. Ind Eng Chem Res 2006, 45, 7126.
5. Bandyopadhyay-Ghosh, S.; Ghosh, S. B.; Sain, M. J Polym Environ 2010, 18, 437.
6. Banik, I.; Sain, M. M. J Reinf Plast Compos 2008, 27, 357.
7. Hu, Y. H.; Gao, Y.; Wang, D. N.; Hu, C. P.; Zu, S.; Vanoverloop, L.; Randall, D. J Appl Polym Sci 2002, 84, 591.
8. Kong, X.; Yue, J.; Narine, S. S. Biomacromolecule 2007, 8, 3584.
9. Chuayjuljit, S.; Sangpakdee, T.; Saravari, O. J Met Mater Miner 2007, 17, 17.
10. Glasser, W. G.; Saraf, V. P. J Appl Polym Sci 1984, 29, 1831.
11. Hatakeyama, H.; Hirose, S.; Nakamura, K.; Hatakeyama, T. Cellulosics: Chemical, Biochemical and Material Aspects; Kennedy, J. F.; Phillips, G. O.; Williams, P. A., Eds. Ellis Harwood: UK, 1993.
12. Hirose, S.; Kobashigawa, K.; Hatakeyama, H.; Gakkaishi, S. I. J Appl Polym Sci 1993, 50, 538.
13. Wilkinson, A. N.; Fithriyah, N. H.; Stanford, J. L.; Suckley, D. Macromol Symp 2007, 256, 65.
14. Saha, M. C.; Kabir, M. E.; Jeelani, S. Mater Sci Eng A 2008, 479, 213.
15. Xu, Z.; Tang, X.; Gu, A.; Fang, Z. J Appl Polym Sci 2007, 106, 439.
16. Giannelis, E. P. Adv Mater 1996, 8, 29.
17. Giannelis, E. P.; Krishnamoorti, R.; Manias, E. Adv Polym Sci 1999, 138, 107.
18. LeBaron, P. C.; Wang, Z.; Pinnavaia, T. J. Appl Clay Sci 1999, 15, 11.
19. Vaia, R. A.; Price, G.; Ruth, P. N.; Nguyen, H. T.; Lichtenhan, J. Appl Clay Sci 1999, 15, 67.
20. Biswas, M.; Sinharay, S. Adv Polym Sci 2001, 155, 167.
21. Ning, L.; Jin, H.; Peter, R. C.; Debbie, P. A.; Jiahui, Y. J Nanomater 2011, 2011, 1.
22. Sinharay, S.; Okamoto, M. Prog Polym Sci 2003, 28, 1539.